Dendronized Perylene Diimide Emitters: Synthesis, Luminescence, and Electron and Energy Transfer Studies

Jianqiang Qu, Jingying Zhang,† Andrew C. Grimsdale, and Klaus Müllen*

Max-Planck-Institut für Polymerforschung, Ackermannweg 10, D-55128 Mainz, Germany

Frank Jaiser, Xiaohui Yang, and Dieter Neher*

Institut für Physik, Universität Potsdam, Am Neuen Palais 10, 14469 Potsdam, Germany

Received March 25, 2004; Revised Manuscript Received August 3, 2004

ABSTRACT: Aggregation of chromophores in the solid state commonly causes undesirable red shifts in the emission spectra and/or emission quenching. To overcome this problem, we have prepared soluble perylenetetracarboxidiimide dyes in which the chromophores are effectively shielded by polyphenylene dendrimers attached in the bay positions. Models show that attachment of the shielding units in the bay position should provide more efficient shielding than attaching them via the imide moieties. The dendrimers possess excellent film-forming properties due to alkyl substituents on their peripheries. The lack of a red shift in emission upon going from solution to the solid state indicates the dendrons suppress interaction of the emissive cores, leading to pure red-orange emission. Single-layer LEDs produce red-orange emission with relatively low efficiency especially for the higher generation dendrons, which is attributed to poor charge conduction. LEDs using blends of the dendrimers and the undendronized dye as a model compound in PVK have been investigated, and a model to extract relative charge injection rates through the dendritic scaffold from the spectral contributions in the EL spectra is developed.

Introduction

Organic materials, both molecular and polymeric, offer substantial advantages over inorganic materials as the emissive components in light-emitting diodes (LEDs), as they are generally more easily processable into devices which thus reduces production costs.[1] Monochromatic LEDs based on organic materials are already entering the commercial marketplace, and ongoing research is concentrated on the development of full color red-green-blue displays using organic materials. One approach is to make use of the extensive research work that has gone into developing organic dyes and pigments, by using such materials as emitters in LEDs.

Perylene-based dyes have long been known as highly photostable pigments or vat dyes.[2] Perylene-3,4,9,10-tetracarboxidiimide (PDI) is the basis for a class of n-type chromophores exhibiting relatively high electron affinity, which possess brilliant colors, strong absorption and fluorescence, and outstanding chemical, thermal, and photochemical stability.[3,4] PDIs have been used as emitting materials in LEDs,[5] but they suffer from two problems which reduce their utility in such devices. First, many PDIs have low solubility, and therefore the preparation of thin film layers has to be carried out by vapor deposition, which is an inferior method for preparing large area films than spin-coating due to its higher cost. An alternative method for preparing thin films containing PDI derivatives would be to blend them with polymers, but this leads to the problem of phase separation. Second, in the solid-state chromophore interactions, such as aggregation, crystallization, and migration, can lead to loss of emission efficiency due to the enhancement of nonradiative decay pathways or red shifts in the emission due to formation of excimers and exciplexes. The first problem can be overcome by covalently incorporating perylene dyes in low concentrations into conjugated polymers, in which efficient energy transfer produces emission only from the dye units.[6] However, the fluorescence efficiencies, and hence maximum device efficiencies, of these copolymers are lower than for the pure dyes, and the chromophore interactions are not completely suppressed.

A very attractive way to solve both these problems simultaneously is to encase the chromophore within a polyphenylene dendrimer shield.[7,8] Dendritic structures offer a unique opportunity to independently vary the physical and electronic properties of organic electronic materials. By connecting dendrons of different generations to a chromophore core, the size of the resulting nanostructure can be controlled, and the chromophore is separated from the surrounding medium, thus preventing undesirable aggregation effects.[9,10] Dendrimers were first introduced in LEDs as hole-transporting materials doped into the emissive host.[11,12] Luminescent dendrimers incorporating emissive cores with phenylenevinylene dendrons have been studied in single-component devices, and the influence of generation on charge transport and light emission has been investigated.[13−15] Polyphenylene dendrimers[16,17] have the advantages of being rigid and shape persistent and have been shown to possess high chemical and thermal stability. We have previously reported the synthesis of materials, e.g. **1**, in which polyphenylene dendrons were attached to the imide structures of a PDI.[18] The absorption and emission spectra of these materials were slightly blue-shifted with those of a model PDI without dendrimer substituents, especially in the solid state, indicating that the dendrimers had efficiently prevented interaction of the chromophores. LEDs using these

† Current address: Key Laboratory for Supramolecular Structure and Materials, Ministry of Education, 119 Jiefang Road, Changchun 130023, P. R. China.

* Corresponding authors. E-mail: muellen@mpip-mainz.mpg.de; neher@rz.uni-potsdam.de.

10.1021/ma0494131 CCC: $27.50
Published on Web 09/30/2004

Scheme 1. Synthesis of the Dendrimers[a]

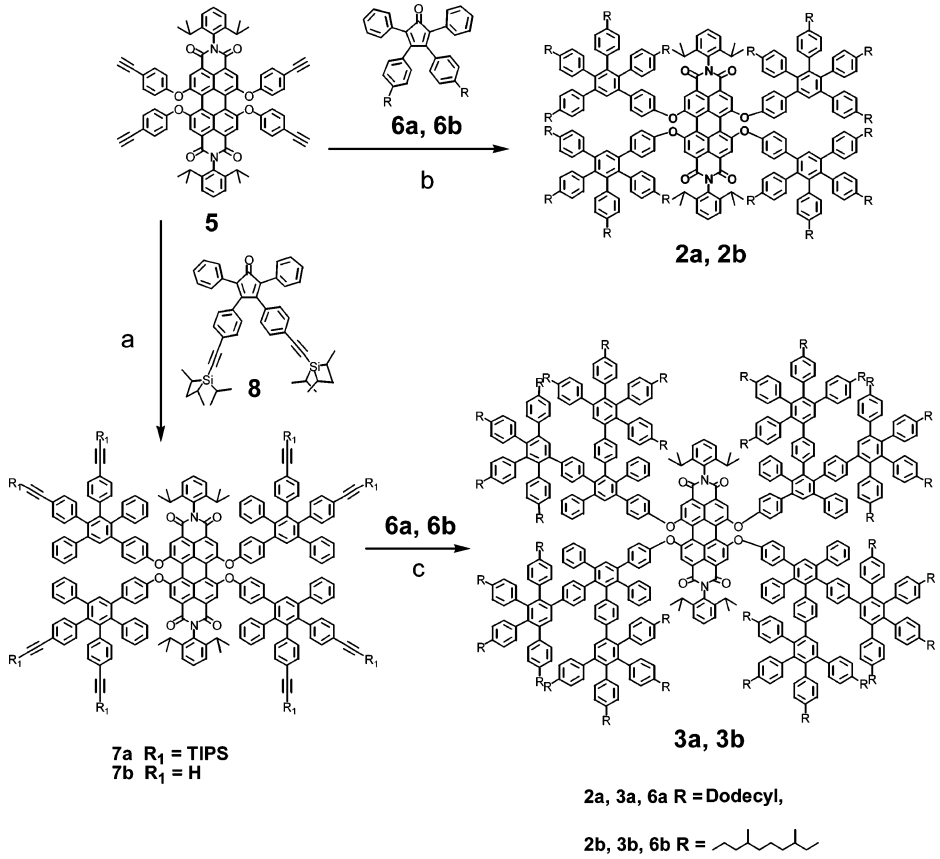

[a] (a) (i) *m*-xylene, 12 h, reflux, 92%; (ii) THF, *n*-Bu_4NF, 30 min, rt, 98%; (b) *m*-xylene, 12 h, reflux, 90%; (c) *m*-xylene, 2 days, reflux, 82%.

materials showed pure red electroluminescence (EL), but with a maximum efficiency of only 0.03 cd/A.[19] The efficiency could be enhanced by blending the dendronized dyes with a blue-emitting polyfluorene, but at the cost of losing some color purity due to emission from the polymer host. However, attachment of dendrimers to the imide moiety of a PDI does not completely shield the chromophore core as only the ends of the molecule are encapsulated. Attachment of dendrimers at the bay positions would be expected to show better shielding of the chromophore, as the core would be more fully encapsulated. As we have recently developed a route by which dendrimer substituents can be attached at the bay position of a PDI,[20] we accordingly prepared dendrimers **2** and **3** in order to test the effect of the greater shielding of the core upon the optoelectronic properties of the PDI.

In this paper we report the synthesis of a novel series of solution processable PDIs substituted in the bay position with polyphenylene dendritic wedges bearing alkyl chains on their outer surface and investigate the effect of both the generation and the different alkyl chains of the dendrimers on their optical and electronic properties. We show that the dendrons effectively shield the chromophores so as to suppress the effects of aggregation upon the fluorescence. The properties of LEDs using these materials both as neat films and as blends in poly(*N*-vinylcarbazole) (PVK) were studied in order to determine the effect of the dendrons upon charge transport. PVK is often used as host material for small-molecular emitters because of its high-energy singlet and triplet states.[21] Furthermore, the contribution of the different possible excitation mechanisms, that is, Förster transfer and direct charge trapping on the dye, and their dependence on the intermolecular distance has been studied by comparing the properties of the dendrimers with the model chromophore **4**.

Results and Discussion

Synthesis and Physical Characterization. The PDI core **5** was prepared as previously reported.[20] Starting from this fluorescent core, a series of PDI-centered polyphenylene dendrimers with straight and branched alkyl chains were synthesized by means of iterative Diels−Alder cycloaddition (Scheme 1). The first-generation dendrimers with 16 alkyl chains **2a** and **2b** were formed by a Diels−Alder reaction of the core molecule **4** with a 6-fold excess of cyclopentadienone **6a** or **6b**[22] in *m*-xylene at 140 °C. Using *m*-xylene as a solvent had the advantage that the product was easily isolated by precipitation from methanol. After filtration, the mixture of product **2a** or **2b** and excess **6a** or **6b** was obtained as a dark-red powder. The pure dendrimer was obtained by repeated precipitation from dichloromethane solution with methanol. For building up the second-generation dendrimer, the first-generation dendrimer bearing ethynyl groups **7b** was prepared by Diels−Alder addition of the cyclopentadienone **8** substituted with ethynyl groups deactivated by silyl substituents, followed by deprotection.[22a] The deprotected dendrimer **7b** was reacted with 12 equiv of **6a** or **6b**, giving the second-generation dendritic chromophore **3a** or **3b**, containing 32 alkyl chains.

Dendrimers **2a**, **2b**, **3a**, and **3b** are all highly soluble in common solvents such as dichloromethane, toluene,

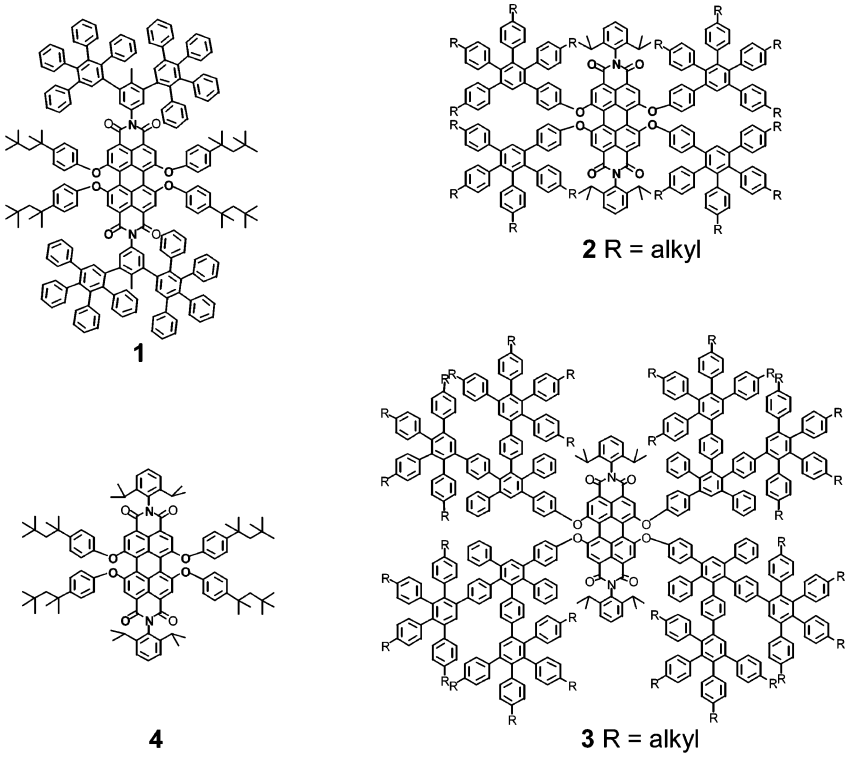

Figure 1. PDIs with dendrimer shields on the imide and at the bay positions.

or THF. Characterization by MALDI−TOF mass spectrometry, elemental analysis, and ^{1}H and ^{13}C NMR spectroscopy was therefore easily accomplished. The experimentally determined and calculated masses for **2a**, **2b**, **3a**, and **3b** agree within the range of accuracy of the instrument. The signals obtained for these macromolecules only showed the molecular ion $[M]^{+}$, and no ions corresponding to partial formation of the dendrons were observed which confirmed their monodispersity (see Supporting Information). As MALDI-TOF-MS measurements allow the detection of potential growth imperfections resulting from unreacted ethynyl groups during the Diels−Alder reaction with the building blocks **6a** or **6b**, this technique was used both for the characterization of the monodisperse dendritic macromolecules described herein as well as for monitoring the dendrimer growth, especially during the synthesis of the second-generation materials **3a** or **3b**, with their longer reaction times.

Because of the polyphenylene structure, these dendrimers have a high thermal stability with primary mass loss occurring at 400 °C. However, their melting points as determined using a melting point apparatus were quite different, occurring at 63, 102, 110, and 143 °C for **2a**, **2b**, **3a**, and **3b**, respectively. These results indicate that both the structure of the groups at the surface and the generation of the dendrimer affect the melting temperature significantly. Branched alkyl chains and higher generation both increase the melting point. An increase of melting point with increasing generation has been previously observed for polyphenylene dendrimers.[17] Polyphenylene dendrimers with branched alkyl chains on the periphery have not been prepared previously. However, the structurally similar hexaphenylbenzenes have higher melting points when substituted with branched alkyl chains than with straight alkyl chains.[23] No glass transition or other phase changes were observed by differential scanning calorimetry (DSC) in any dendrimer up to the decomposition temperature.

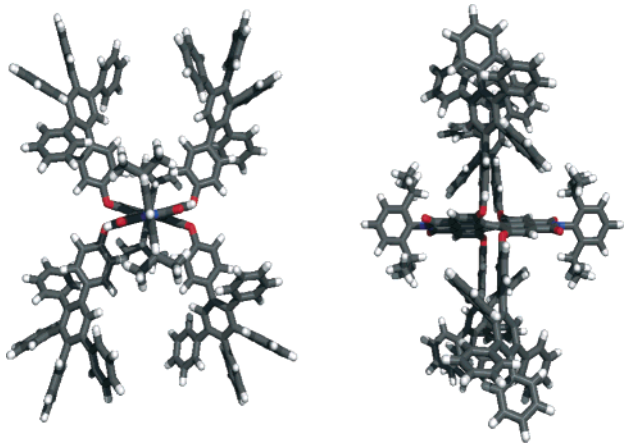

Figure 2. 3D model of the first-generation dendronized PDI without alkyl chains at periphery.

The structure of the first-generation dendrimer without alkyl chains was optimized using the MM2 (MM+) force field geometry optimization program HyperChem 6.0 (Hypercube Inc.). A force field method was preferred over the application of quantum mechanics methods due to the prohibitively large number of atoms in the dendritic molecule, and the perylene core was optimized by using the semiempirical PM3 method. Furthermore, optimization of the whole dendritic system was performed by combining four first-generation dendrons with the perylene core and minimizing the whole system. Molecular modeling suggests that in dendrimers **2a**, **2b**, **3a**, and **3b** the chromophores are completely surrounded by the dendritic shells. As shown in Figure 2, the two naphthalene units of the perylene in the simulated structure of the first-generation dendrimer without alkyl chains are strongly twisted at the bay position with a torsional angle around 28° between

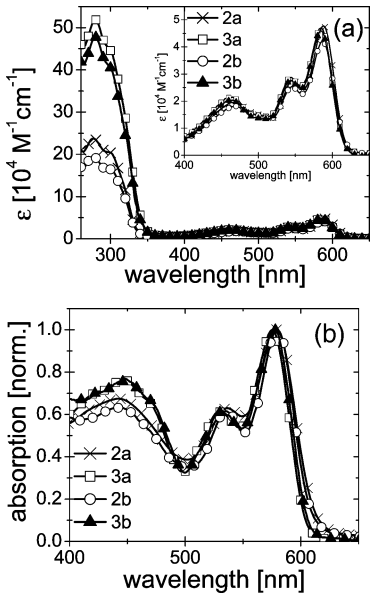

Figure 3. UV/vis spectra of dendrimers **2a**, **2b**, **3a**, and **3b** (a) in chloroform and (b) in the film on quartz.

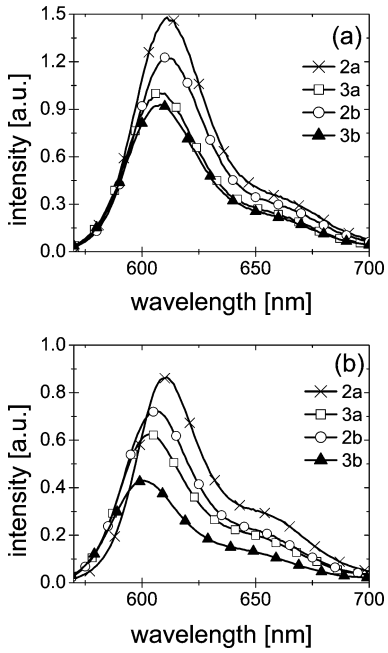

Figure 4. PL spectra of dendrimers **2a**, **2b**, **3a**, and **3b** (a) in chloroform and (b) thin films (excited at 560 nm).

them, which is in good agreement with the crystal structure of a similar molecule.[24] This simulation also shows the phenoxy groups to be arranged nearly perpendicular to the perylene ring. The size of the compounds increases with the generation of dendrimer—the diameters being 3.7 nm for the first-generation dendrimer without alkyl chains and 5.3 nm for the second-generation dendrimer without alkyl chains (whose optimized structure is not shown). Obviously, the perylene core is efficiently shielded by the dendrons which can thus inhibit aggregation of the perylene units.

Optical Properties. To determine the effect of the dendritic shell on the PDI chromophore, the optical properties of **2a**, **2b**, **3a**, and **3b** were investigated. Their UV/vis absorption spectra in chloroform exhibit two regions as shown in Figure 3A. The first absorption is due to the central chromophore, which displays three maxima at around 585, 543, and 465 nm. The second absorption band at much shorter wavelength is from the dendritic framework (∼278 nm), which consists of strongly twisted benzene units. We found that the ratio of absorption of the dendron to that of the core increased as the dendrimer generation increased due to the increase in the number of benzene units. Because of the out-of-plane twisted molecular structure of polyphenylene dendrons, the dendronized PDIs have a high solubility in various organic solvents and form good films when spin-coated onto quartz. The solid-state absorption spectra of these dendrimers are presented in Figure 3B. These dendrimers **2a**, **2b**, **3a**, and **3b** display distinct vibronic fine structure of PDI core and exhibit similar spectra in film in comparison to that in the solution. The maxima of absorption spectra in the solid state are little different from those in solution (around 7 nm blue shift). The photoluminescence (PL) spectra of dendrimers **2a**, **2b**, **3a**, and **3b** are measured in chloroform solution and in thin films, with excitation at 560 nm as shown in Figure 4. The PL spectra of these dendrimers, like the absorption spectra, all exhibit a clear vibronic structure, which suggests the absence of pronounced intermolecular interactions. For the solution spectra, the maxima are located at 611, 608, 610, and 608 nm for **2a**, **3a**, **2b**, and **3b**, respectively, while the corresponding maxima for the films are at 611, 604, 606, and 601 nm, respectively. The PL spectra undergo a small blue shift (2−3 nm in the solution and 5−7 nm in the solid state) with increase of the generation of the dendrimer, which is ascribed to the greater isolation of the chromophores with increasing generation. This is contrast to the behavior of the dyes such as **1** dendronized at the imide, where no such blue shift was observed.[18] The PL spectra of the films are also similar to those of the solutions with even the first-generation dendrimers showing no significant red shift in the film. By contrast, we have previously reported that a tetraaryloxy PDI without dendron substituents exhibits a marked red shift in its solid-state absorption and emission spectra,[19] similar to that previously observed for other dyes,[25] which is generally attributed to interactions such as $\pi-\pi$ stacking between the chromophores. These spectra also suggest that aggregation, crystallization, and migration of the chromophores are reduced in the dendrimers and indicate that even the first-generation dendrimers can effectively suppress $\pi-\pi$ stacking between PDI chromophores, as was previously seen for dendrimer **1**.[18]

Light-Emitting Diodes. To determine the effect of the dendrimer shells on the electronic properties of the dyes, LEDs were constructed. Because the melting temperature of **2a** is below the likely maximum operating temperature of an LED (ca. 80 °C), only **2b**, **3a**, and **3b** were used as emitting materials to prepare devices, and their electroluminescence (EL) spectra are presented in Figure 5. A hole-transporting layer of PEDOT was used. The EL spectra are similar to the PL spectra, suggesting that both types of luminescence arise from the same excited state of the PDI core. Some fine structure is observed in the EL spectra. The maxima of the EL spectra are at 596, 611, and 598 nm for **3a**, **2b**, and **3b**, respectively. The EL spectrum of the second-generation dendrimer **3b** is slightly blue-shifted compared to the first-generation dendrimer **2b**, which is in agreement with the PL measurements. Surprisingly, the second-generation materials **3a** and **3b** show a small blue shift (∼10 nm) in the EL spectra compared to the PL spectra. This phenomenon has been observed in

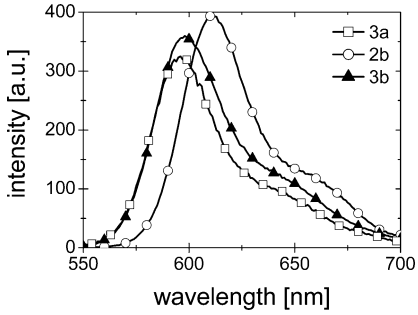

Figure 5. EL spectra of dendrimers **2b**, **3a**, and **3b**.

other organic materials such as poly(*p*-phenylene),[26] poly(*p*-phenylenevinylene),[27] and poly(3-cyclohexylthiophene).[28] Several effects such as self-absorption phenomena in the LED structure might account for this spectral shift.

All the devices displayed diode-like characteristics (see Supporting Information). The turn-on voltage of the devices using the second-generation dendrimers (9 V) was higher than those of the corresponding devices using the first-generation dendrimer (4 V). This effect is presumably due to the poorer charge transport properties of the second-generation dendritic wedges,[14] which lowers the current density and EL intensity of the devices simultaneously. Their brightnesses, current densities, and efficiencies were low, e.g. 0.14 cd/A at 10 V and 3.66 mA/cm^2 for the device based on **2b**. These efficiencies are comparable with those observed for the PDIs bearing dendrimer groups on the imide structures.[19] Lower brightness and current density was observed for the devices based on second-generation dendrimers, an effect which was also seen for the PDIs with dendrimers on the imides,[19] which again suggests that the extended dendrimer structure significantly decreases the transport of charge to the core.

Blends of Dendrimers with PVK:PBD Matrix. The results presented above have shown that increasing the thickness of the dendritic scaffold strongly affects charge transport in layers prepared solely from dendrimers. However, diodes fabricated via solution-processing often contain an emissive dye blended into an appropriate charge-transporting polymer matrix. In fact, highly efficient electrophosphorescent diodes using iridium complexes have been reported recently.[29] In these blended layers, excitation of the dye occurs either via the formation of excitons on the host followed by energy transfer to the dendron core or via direct charge carrier trapping on the dye.

In the following we show how the dendrimer shell thickness affects the efficiency of these processes and provide a simple model to extract the correlation between electron-transfer rates and generation. For these experiments, poly(*N*-vinylcarbazole) (PVK) blended with 30 wt % of the electron-transporting compound 2-(4-biphenylyl)-5-(4-*tert*-butylphenyl)-1,3,4-oxadiazole (PBD) has been used as the matrix. In combination with a phosphorescent iridium dye, efficient transfer of energy and charges to the guest has been reported, resulting a large quantum efficiencies.[21,29] In the PL and EL experiments, only small concentrations of the dendrimers in the matrix have been used for two reasons: first, the absorption of PVK overlaps with the absorption spectrum of the perylene diimide. Therefore, the chromophore concentration must be as small as possible to avoid direct excitation of the dye in the energy-transfer

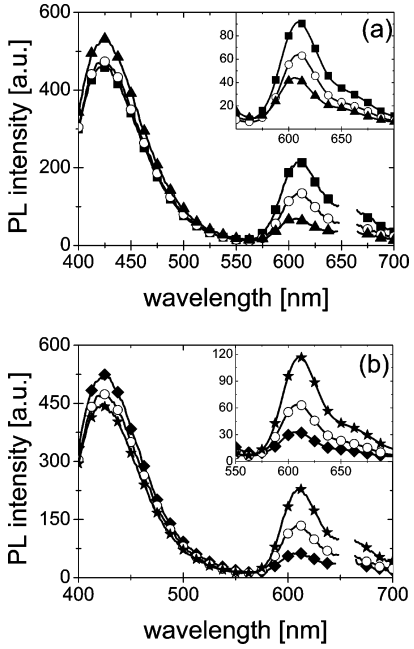

Figure 6. (a) PL spectra of PVK−PBD blended with 500 ppm of **4** (squares), **2b** (circles), and **3b** (triangles) at an excitation wavelength of 330 nm (excitation of the PVK matrix). The gap at 660 nm cuts out the second-order peak of scattered excitation light. (b) PL spectra of PVK−PBD matrix doped with increasing concentration of **2b**. Diamonds, circles, and stars show spectra measured at concentrations of 150, 500, and 1500 dye molecules per million PVK repeating units, respectively. The insets shows PL spectra of the same films upon direct excitation of the dendrimers at 500 nm.

experiments. Second, the perylene diimide core acts as a charge trap in the PVK:PBD matrix. Therefore, higher concentrations of the dendrimers in the matrix will significantly alter the electrical properties of the devices.

Figure 6a shows the photoluminescence spectra of films containing 500 ppm (given in terms of number of dye molecules relative to the number of PVK repeat units) of **4**, **2b**, and **3b**. The spectra were measured either upon excitation of the matrix at 330 nm or with direct excitation of the dye at 500 nm (inset). Note that a constant molar content of the molecules means that the weight fraction increases with increasing generation. For direct dye excitation, the spectra resemble those for the dilute solutions and the pure dendrimer films as shown in Figure 4. Note that for the same molar content of dye in the PVK:PBD matrix the emission intensity decreases with increasing generation, as was observed in solution and in the pure films. A similar correlation between the fluorescence quantum yield and generation was earlier reported for a structurally related perylene diimide dendrimer. This was explained by new nonradiative deactivation pathways introduced by the polyphenylene dendrons.[10,18]

Upon matrix excitation at 330 nm, the spectra show a broad and intense PVK:PBD exciplex emission (up to a wavelength of 560 nm) and a second emission band located at about 605 nm originating from the PDI compounds. Again, the PDI emission spectrum in the matrix resembles the shape of the solution and pure film PL. When normalized to matrix emission, the red contribution drops to 60% and 27% of the value of **4** for **2b** and **3b**, respectively, for the same molar concentration. This is attributed to the fact that the dendronic shell increases the distance between host and PDI core. Because the fraction of dye molecules in the films is

rather low, they do not significantly contribute to the absorption at 330 nm (as confirmed by absorption spectra measured for all generations). Thus, almost all excitons will be formed on the matrix. Therefore, the excitation of the dye requires exciton transfer between the matrix to the dye by Förster energy transfer. As the host-to-guest distance increases with generation, the rate of Förster transfer is expected to decrease with increasing generation. The efficiency of Förster transfer will be discussed in greater detail later.

Figure 6b shows exemplary PL emission spectra of films containing different amounts of **2b**. Several effects can be seen: First, as expected, the dye emission increases with increasing dye concentration. However, this increase is not completely linear with dye content (or with dye absorption), indicating that nonemissive aggregates are formed at higher concentrations even for the dendronized chromophores. Concurrently, the matrix PL decreases noticeably at higher dye concentrations. Apparently, the dendron shell cannot fully prevent the dye from the formation of nonemissive aggregates. Similar measurements of films containing the model compound or second-generation dendrimers (not shown) show that this effect is more pronounced in films containing **4** and nearly absent in films of **3b**.

Upon direct excitation (inset), the same behavior is observed: with increasing dye content, the emission increases sublinearly with dye concentration. Second, a slight red shift of the emission maximum with concentration is observed. Again, this effect is more pronounced for films containing **4** and virtually absent for **3b**. Because of the low dye content, filter effects can be excluded as a possible explanation for this red shift. Note that Lupton et al. attributed an emerging red tail to the formation of excimers.[14] These results suggest that although interchromophore interactions are reduced by dendronization, as previously suggested by the small red shift between the solution and solid-state PL spectra, they are not totally suppressed even with the second-generation dendrons. To prevent significant concentration quenching, all further investigations were performed at low dye concentrations.

The rate of Förster transfer from an isolated donor (that is, an excited PVK:PBD host state) to a single acceptor (here: PDI dendrimer guest molecule) is given by[30]

$$k_F = \frac{1}{\tau}\left(\frac{R_0}{R}\right)^6 \tag{1}$$

Here, τ is the lifetime of the undisturbed host, R the host-to-guest distance, and R_0 the Förster transfer radius. (The Förster radius is the host-to-guest distance for which the deactivation of the host molecule by Förster transfer and by fluorescence decay become equally probable.) R_0 can be calculated from the PL quantum yield of the undisturbed host, the refractive index of the material ($n = 1.7$ for PVK), and the spectral overlap between the host fluorescence and the guest absorbance. Using an estimated PL quantum yield of 0.094 for the PVK:PBD blend,[31] the calculated Förster radius increases slightly from about 2.4 to 2.6 nm with generation.

Equation 1 is valid only for the energy transfer between a single excited host molecule in the vicinity of an isolated guest. In the blend films under investigation, host and guest molecules are statistically distributed in the sample. In a recent paper, Bulovic et al. derived an equation, taking into account the interaction between an excited host molecule and several randomly distributed guests.[32] Most important, the minimum distance between the excited energy donor and an acceptor is given by the sum of the respective molecular radii, which was assumed to be identical in ref 32. Using different radii, namely a and b for the host and the guest molecule, respectively, the following equation can be derived for the total transfer rate:

$$k_{F,tot} = \frac{4\pi N_A \rho_{host} Q}{3\tau M_{host}} \frac{{R_0}^6}{(a+b)^3} \tag{2}$$

Here, Q is the molar fraction of guest molecules in the host matrix of mass density ρ_{host} and M_{host} is the molar mass of the host. Thus, the efficiency of Förster transfer becomes

$$\eta_F = \frac{k_{F,tot}}{k_{F,tot} + \frac{1}{\tau}} = \frac{1}{1 + \frac{3M_{host}}{4\pi N_A \rho_{host} Q} \frac{(a+b)^3}{{R_0}^6}} \tag{3}$$

According to recent spectroscopic studies, the excited state of the PVK:PBD matrix is an PVK:PBD exciplex,[33] with an estimated radius of $a = 1.1$ nm. Assuming a mass density of the polymer film of about 1 g/cm^3 and using $b = 1.1$, 1.9, and 2.7 nm for **4**, **2b**, and **3b**, respectively, Förster transfer efficiencies of 10.2%, 5.9%, and 3.2% are obtained for $Q = 500$ ppm.

According to these estimates, the Förster transfer efficiency drops roughly by a factor of 1.8 for each dendron shell added. The observed spectra show that the red emission drops by a factor of 2 for each generation (Figure 6a). However, note that the emission intensity of the dye upon direct excitation decreases by a factor of ca. 1.5 with each generation. This factor is assumed to reflect a decrease of the average fluorescence quantum efficiency of the dye in the PVK:PBD matrix as mentioned earlier. Hence, the Förster transfer efficiency can be estimated to decrease by a factor of about 1.3 for each dendron shell added, which is slightly smaller than the calculated values. However, note that the host emission intensity decreases roughly by 10% when going from **3b** to **4**, which agrees roughly with the above estimate. Also, only the aromatic part of the dendritic shell has been taken into account, while the volume taken up by the solubilizing alkyl chains was neglected. Another reason for the low transfer rates observed might be that the dendritic shell as well as the substituents introduce significant disorder in the adjacent PVK:PBD matrix, thus reducing the probability for excimer formation in close proximity to the dendrimer.

Note that the considerations described above neglect the diffusion of excitons between host molecules toward the guest. It has been shown that the diffusion of excitons significantly enhances the energy transfer rate between a conjugated polymer host and a dye.[34] On the other hand, the energy transfer between a PVK:PBD matrix and an iridium dye could be well understood on the basis of the conventional Förster transfer theory.[35] Most likely, the excited exciplex state is rather immobile, and energy migration is preferentially to the energy-accepting dye. In agreement with this interpretation, the dependence of the energy transfer rate on

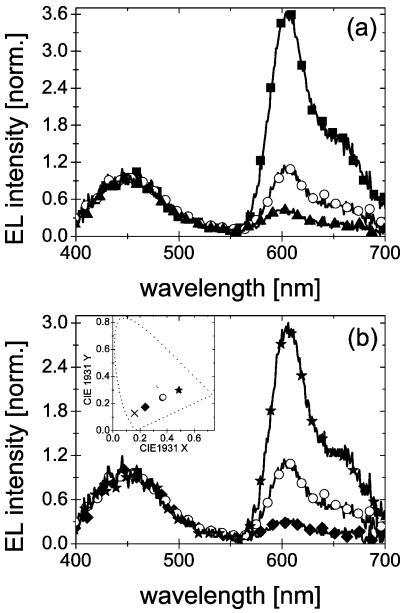

Figure 7. (a) Normalized EL spectra of PVK:PBD blended with 500 ppm **4** (squares), **2b** (circles), and **3b** (triangles) at an operating current density of 20 mA/cm^2. (b) EL spectra devices with the PVK:PBD matrix doped with **2b** at a concentration of 250 (diamonds), 500 (circles), and 1000 ppm (stars). The inset shows the according CIE color coordinates at a driving voltage of 10 V including the pure matrix (cross) for comparison.

generation was far more pronounced for the blend of a related PDI derivative in a polyfluorene matrix, even though this donor−acceptor pair has a similar Förster radius of 2.9 nm.[19] In this case, energy transfer occurs from the singlet exciton on the PF chains, and no excimer formation is involved in this process.

EL spectra of films containing 500 ppm **4**, **2b**, and **3b** are shown in Figure 7a. All spectra were recorded at a driving current density of 20 mA/cm^2. Compared to the corresponding PL spectra, the red contribution from PDI is enhanced for all three blends. At the same time, the decrease in red dye emission with generation is more pronounced. Both tendencies indicate that charge trapping on the dyes plays a major role in the excitation of the dye in EL. This is not surprising considering the HOMO and LUMO levels of the matrix compared to the dyes. The HOMO and LUMO of PVK are −5.8 eV and −2.2 eV, respectively.[21] For the electron-transporting PBD, LUMO positions of −2.0 eV and −2.6 eV and a HOMO energy of −6.3 eV have been reported.[36] For structurally similar PDI dendrimers, HOMO and LUMO levels of −5.4 eV and −3.6 eV to −3.4 eV vs Ag/AgCl have been measured.[19] Apparently, the dye in the PVK:PBD matrix acts as a deep trapping site for electrons and a weaker hole trap.

Given the rather low dye concentration used here, charges will be almost exclusively injected into the matrix transport levels. Excitation of the dye will then occur by the formation of excitons (excimers) on the host and subsequent Förster transfer to the dye and by tunneling of both carriers from the polymer matrix to the dye. Because the tunneling probability decreases with e^{-2R}, we expect that the insulating dendron shell has a larger influence on the trapping process than on the Förster transfer.

In Figure 7b, EL spectra of blend films containing **2b** in different concentrations are shown. As in PL, the red contribution increases slightly sublinear with increasing

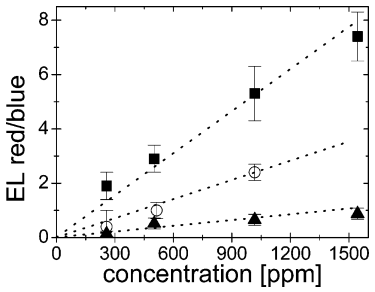

Figure 8. Ratio of peak red emission intensity and the peak blue emission for EL, driven at current density of 20 mA/cm^2. Squares, circles, and triangles mark blends with **4**, **2b**, and **3b**, respectively. The error bars indicate the device scattering that is especially high for devices with model compound **4**.

dye content. Similar spectra were obtained for films containing **4** and **3b** (not shown).

We have analyzed the ratio of the red and blue emission contributions in EL, compared to that in PL, to obtain information on the different contributions of Förster transfer and charge trapping for the different dendrimers in EL. These ratios are shown in Figure 8 as a function of concentration for all three dendrimers. When going from model **4** to **2b**, there is a steep decrease in the ratio while the decrease is less pronounced when going from **2b** to **3b**. For all generations, the red-to-blue ratio in EL is much larger than in PL, namely a factor of 6−8 for **4**, up to 6 for **2b**, and 4 for **3b**.

As discussed above, the photoluminescence red emission is the result of Förster transfer. Because of the small amount of dye in the system, virtually all excitons will be formed on the PVK:PBD matrix in the PL experiments. Prior to reemission of a photon, a certain fraction b of the excitation will be transferred to the dye. Thus, a fraction $(1 - b)\phi_{host}$ of photons will be emitted by the matrix and a fraction $b\phi_{guest}$ by the dye. Here, ϕ_{host} and ϕ_{guest} are the PL quantum yields of the host and the guest, respectively.

In electroluminescence, almost all charges will be injected onto the PVK:PBD matrix. Because of the large difference of the respective LUMO levels, the dye is assumed to form an efficient electron trap with trapping coefficient γ. Subsequent hole trapping by the negatively charged dye (described by the coefficient γ_T) will lead to the emission of excitons from the dye. Then, the rate equation for the trapping and recombination of electrons on the dye becomes

$$\frac{dT_e^-}{dt} = \gamma n(t)[T_e - T_e^-(t)] - \gamma_T T_e^-(t)\, p(t) \qquad (4)$$

Here, T_e is the total number density of dyes in the matrix, $T_e^-(t)$ is the density of negatively charged dye molecules, and $n(t)$ and $p(t)$ are the electron and hole densities on the matrix, respectively. Note that the possibility of (thermal) detrapping of electrons was excluded because of the large difference between the guest and host LUMO positions. Under steady-state conditions, $dT_e^-/dt = 0$. Assuming that only few dye molecules are populated ($T_e \gg T_e^-$), we obtain

$$\gamma n T_e = \gamma_T T_e^- p \qquad (5)$$

In parallel, excitons will form on the matrix with a rate $\gamma_R n(t)p(t)$, with γ_R being the coefficient for electron−hole recombination on the matrix. Taking into account

Förster transfer to the guest, the number of photons emitted per second by the host is $(1 - b)\phi_{host}\gamma_R np$. On the other hand, the dye emission rate is determined by two contributions, $b\phi_{guest}\gamma_R np$ and $\gamma_T T_e^{-} p$.

Thus, the PL and EL emission ratios are given by

$$\left.\frac{I_{guest}}{I_{host}}\right|_{PL} = \frac{\phi_{guest}}{\phi_{host}} \frac{b}{1-b} \tag{6}$$

$$\left.\frac{I_{guest}}{I_{host}}\right|_{EL} = \frac{\phi_{guest}}{\phi_{host}} \frac{\gamma n T_e + \gamma_R npb}{\gamma_R np(1-b)} = \frac{\phi_{guest}}{\phi_{host}} \frac{\gamma n T_e}{\gamma_R np(1-b)} + \left.\frac{I_{guest}}{I_{host}}\right|_{PL} \tag{7}$$

Thus

$$\left.\frac{I_{guest}}{I_{host}}\right|_{EL} - \left.\frac{I_{guest}}{I_{host}}\right|_{PL} = \frac{\gamma}{\gamma_R} \frac{\phi_{guest}}{\phi_{host}} \frac{T_e}{p(1-b)} \tag{8}$$

and the difference between the EL and PL emission ratios is a measure for the coefficient γ describing electron trapping on the chromophore. In the following analysis, intensity ratios measured at a constant current density of 20 mA/cm^2 were compared for the same molar dye concentrations. Since the current/voltage characteristics were almost independent of generation and concentration in the range studied here, this corresponded to similar driving fields. We have also assumed that the fluorescence quantum yield ϕ_{guest} is the same for all generations and that the Förster transfer ratio b for the different generations is small (as suggested by the small drop of the PVK emission shown in Figure 6). Using the data shown in Figure 8, we conclude that the trapping coefficient decreases by a factor of about 3 for each added dendron shell. Moreover, the factor drops further to ca. 2 when taking into account the decrease in fluorescence quantum yield with generation as suggested by the data shown in Figures 4b and 6a. This factor is surprisingly small, having in mind the significant change in the thickness of the dendronic shell with increasing generation. In contrast, the effect of increasing generation on the properties of LEDs with pure dendrimer layers was very pronounced as described above. However, as can be seen in Figure 2, the dendritic shell is not perfectly spherical. Therefore, the penetration of the shell by e.g. PBD might be possible, enabling rather efficient electron transfer from the PVK:PBD matrix to the core of the dendrimers.

Note that our conclusions from the EL experiments are in good agreement with the results of charge transport studies on conjugated dendrimers with a iridium-based phosphorescent core and phenylene dendrons.[37] Here, the zero-field mobility of pure layers of the second-generation dendrimer was measured to be ca. 3 times lower than that of the first-generation compound. Also, the field dependence of the mobility was quite the same for the two compounds, indicating that spatial disorder in layers prepared from these compounds is not dependent on the generation. Therefore, we presume that the effect of the generation on the charge carrier mobility as reported by Markham et al.[37] and on the EL spectra as discussed here has a common origin, namely the rate for electron transfer through the dendritic shell.

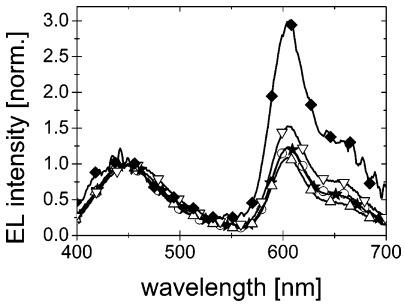

Figure 9. Normalized EL spectra of devices doped with 250 ppm **2b** and different injection electrodes: ITO−polymer−LiF−Ca−Al (diamonds), ITO−PANi−polymer−LiF−Ca−Al (lower triangles), ITO−PEDT−polymer−LiF−Ca−Al (circles), ITO−PEDT−polymer−Ca−Al (stars), and ITO−PEDT−polymer−Al (upper triangles). All spectra (except for the ITO-only device, which showed very weak emission) have been measured at comparable host emission intensities.

One particular prediction of eq 8 is that the guest emission normalized to the host emission intensity is inversely proportional to the concentration of free holes in the device. Thus, an increase in the hole density should decrease the red contribution. In accordance with this picture, we observed that the red emission contribution decreased continuously with increasing bias. This effect was even more pronounced when blending PDI dendrimers into a polyfluorene host. We further observed that the choice of the charge-injecting electrodes has a pronounced influence on the EL spectra (Figure 9) on the injection barrier for holes. These spectra have been measured at comparable host emission intensities, and therefore, the product of the densities of free holes and electrons should be about the same. Hence, the relative red emission contribution is expected to decrease when lowering the barrier for hole injection (which increases the hole density) and to increase when decreasing the barrier for electron injection (which decreases the hole density for comparable host emission intensities).

In our experiments, the ITO−PEDOT anode, whose work function is ca. 5.2 eV, leaves a relatively small barrier for hole injection. Devices with O_2-plasma-treated ITO as the anode (work function of ca. 4.8 eV) have a significantly higher red emission contribution. When PEDOT is replaced by PANi, the red contribution is slightly larger compared to a PEDOT-containing device but significantly smaller than for the ITO-only devices. Interestingly, changing the cathode work function affected the spectra only slightly. Nevertheless, there was a slight increase in the red emission contribution with decreasing electron barrier, as predicted by eq 8.

Conclusions

New PDI derivatives bearing alkyl-substituted pentaphenylene first- and second-generation dendrons at the bay positions have been prepared. These materials show good solubility and film-forming properties and display strong red-orange photoluminescence with reduced chromophore interactions, indicating that the dendritic shells shield the emissive cores. Weak concentration quenching effects were observed, indicating that even the second-generation dendrimers do not totally suppress the interchromophore interactions. The use of branched alkyl chains was found to increase the melting points of the materials but to have no significant

effect on their optical properties. LEDs fabricated with these materials showed low efficiencies, especially with the second-generation dendrimers, which is attributed to poor charge transport through the dendritic shell. These derivatives have been further used to probe the energy and charge transfer in a PVK:PBD-based charge transporting host. Our data show that the Förster transfer rate decreases by a factor 1.3−1.8 with generation, which agrees well with the predictions by the Förster transfer theory. Further, the spectral contributions in the EL spectra of devices based on the blend layers have been analyzed to estimate the changes in the electron-transfer coefficient with increasing dendritic shell thickness. It is concluded that this coefficient decreases by a factor of 2−3 with every generation. This rather weak decrease in the estimated electron-transfer rate suggests that individual PBD molecules or even PVK repeat units penetrate into the dendrimer shell.

Experimental Section

OLED Fabrication. LEDs were fabricated on ITO substrates which had been ultrasonicated sequentially in detergent, deionized water, toluene, acetone, and 2-propanol and then treated with O_2 plasma for 10 min before use.

(a) Dendrimer-Only Devices. A hole-injecting layer (70 nm) of poly(3,4-ethylenedioxythiophene) doped with poly(styrenesulfonate) (PEDOT:PSS, Aldrich Corp.) was deposited by spin-coating from an aqueous solution (1.3 wt %) onto the ITO substrates and cured at 100 °C for 30 min under vacuum. Then an emitting layer of the PDI dendrimer (ca. 100 nm) was spin-coated from $CHCl_3$ solution (15 mg/mL). An aluminum cathode (120 nm) was then vacuum-deposited (5×10^{-6} mbar) through a mask; the area of each pixel was about 7 mm^2. Current−voltage measurements were carried out using a Keithley 236 source-measure unit while detecting the electroluminescence by photomultiplier tube. The thickness of the films was measured by a surface profilometer.

(b) PVK−Dendrimer Blend Devices. A layer (20 nm) of poly(ethylenedioxythiophene) doped with poly(styrenesulfonate) (PEDOT:PSS, Baytron P, H.C. Starck) was spin-coated on top of the indium tin oxide (ITO) anode. On top of that, a 70 nm thick layer of PVK ($M_n = 11 \times 10^6$ g/mol, Aldrich) containing 30 wt % electron-transporting 2-(4-biphenylyl)-5-(4-*tert*-butylphenyl)-1,3,4-oxadiazole (PBD) (Aldrich) from chlorobenzene solution was spin-coated. Varying amounts of the three dendrimer generations (**8**, **2b**, **3b**) were added to the solution prior to spin-coating. For electrical characterization, an ultrathin LiF layer followed by 20 nm Ca and 100 nm Al was evaporated through a shadow mask. The active area of the devices was 0.15 cm^2. Photoluminescence spectra were recorded for polymer films on glass substrates using a Perkin-Elmer LS-50 luminescence spectrometer. Electrical characterization was done with a Keithley 2400 source meter. Luminance and color coordinates were measured with a Minolta CS-100 A chromameter, and EL spectra were recorded using an charge-coupled device fiber spectrometer (Ocean Optics). The film thickness was measured with a Dektak 3 profilometer.

Acknowledgment. This research was supported by the Max-Planck-Society, the TMR European Research Program through the SISITOMAS project, the Volkswagen-Stiftung, the Bundesministerium für Bildung und Forschung, the BASF AG, and the Fonds der Chemischen Industrie.

Supporting Information Available: Full experimental details for synthesis of dendrimers **2** and **3**; *I*−*V* curves for single-layer devices using **2a**, **3a**, and **3b**. This material is available free of charge via the Internet at http://pubs.acs.org.

References and Notes

(1) Bernius, M. T.; Inbasekaran, M.; O'Brien, J.; Wu, W. S. *Adv. Mater.* **2000**, *12*, 1737.
(2) Fabian, J.; Zahradnik, R. *Angew. Chem., Int. Ed. Engl.* **1989**, *28*, 677.
(3) Lee, S. K.; Zu, Y.; Herrmann, A.; Geerts, Y.; Müllen, K.; Bard, A. J. *J. Am. Chem. Soc.* **1999**, *121*, 3513.
(4) Quante, H.; Geerts, Y.; Müllen, K. *Chem. Mater.* **1997**, *9*, 495.
(5) (a) Jiang, X. Z.; Liu, Y. Q.; Liu, S. G.; Qiu, W. F.; Song, X. Q.; Zhu, D. B. *Synth. Met.* **1997**, *91*, 253. (b) Ranke, P.; Bleyl, I.; Simmerer, J.; Haarer, D.; Bacher, A.; Schmidt, H. W. *Appl. Phys. Lett.* **1997**, *71*, 1332. (c) Kalinowski, J.; Marco, P. D.; Fattori, V.; Giuletti, L.; Cocchi, M. *J. Appl. Phys.* **1998**, *83*, 4242.
(6) Ego, C.; Marsitzky, D.; Becker, S.; Zhang, J.; Grimsdale, A. C.; Müllen, K.; MacKenzie, J. D.; Silva, C.; Friend, R. H. *J. Am. Chem. Soc.* **2003**, *125*, 437.
(7) Weil, T.; Reuther, E.; Müllen, K. *Angew. Chem., Int. Ed.* **2002**, *41*, 1900.
(8) Qu, J.; Liu, D.; De Feyter, S.; Zhang, J.; De Schryver, F. C.; Müllen, K. *J. Org. Chem.*, submitted.
(9) Gronheid, R.; Hofkens, J.; Kohn, F.; Weil, T.; Reuther, E.; Müllen, K.; De Schryver, F. C. *J. Am. Chem. Soc.* **2002**, *124*, 2418.
(10) Liu, D.; De Feyter, S.; Cotlet, M.; Stefan, A.; Wiesler, U.-M.; Herrmann, A.; Grebel-Koehler, D.; Qu, J.; Müllen, K.; De Schryver, F. C. *Macromolecules* **2003**, *36*, 5918.
(11) Kuwabara, Y.; Ogawa, H.; Inada, H.; Noma, N.; Shirota, Y. *Adv. Mater.* **1994**, *6*, 677.
(12) Sainova, D.; Miteva, T.; Nothofer, H. G.; Scherf, U.; Glowacki, I.; Ulanski, J.; Fujikawa, H.; Neher, D. *Appl. Phys. Lett.* **2000**, *76*, 1810.
(13) Halim, M.; Pillow, J. N. G.; Samuel, I. D. W.; Burn, P. L. *Adv. Mater.* **1999**, *11*, 371.
(14) Lupton, J. M.; Samuel, I. D. W.; Beavington, R.; Burn, P. L.; Bässler, H. *Adv. Mater.* **2001**, *13*, 258.
(15) Lupton, J. M.; Samuel, I. D. W.; Beavington, R.; Frampton, M. J.; Burn, P. L.; Bässler, H. *Phys. Rev. B* **2001**, *63*, 155206.
(16) Berresheim, A. J.; Müller, M.; Müllen, K. *Chem. Rev.* **1999**, *99*, 1747.
(17) Wiesler, U. M.; Berresheim, A. J.; Morgenroth, F.; Lieser, G.; Müllen, K. *Macromolecules* **2001**, *34*, 187.
(18) Herrmann, A.; Weil, T.; Sinigersky, V.; Wiesler, U.-M.; Vosch, T.; Hofkens, J.; De Schryver, F. C.; Müllen, K. *Chem.—Eur. J.* **2001**, *7*, 484.
(19) Meisel, A.; Herrmann, A.; Miteva, T.; Nothofer, H.-G.; Scherf, U.; Müllen, K.; Neher, D., manuscript in preparation.
(20) Qu, J.; Pschirer, N. G.; Liu, D.; Stefan, A.; De Schryver, F. C.; Müllen, K. *Chem.—Eur. J.* **2004**, *10*, 528.
(21) Kawamura, Y.; Yanagida, S.; Forrest, S. R. *J. Appl. Phys.* **2002**, *92*, 87.
(22) (a) Ito, S.; Wehmeier, M.; Brand, J. D.; Kübel, C.; Epsch, R.; Rabe, J. P.; Müllen, K. *Chem.—Eur. J.* **2000**, *6*, 4327. (b) Fechtenkötter, A.; Tchebotareva, N.; Watson, M.; Müllen, K. *Tetrahedron* **2001**, *57*, 3769.
(23) Fechtenkötter, A. PhD Thesis, University Mainz (Germany), 2001.
(24) Würthner, F.; Sautter, A.; Thalacker, C. *Angew. Chem., Int. Ed.* **2000**, *39*, 1243.
(25) (a) Hädicke, E.; Graser, F. *Acta Crystallogr.* **1986**, *C42*, 189, 195. (b) Duff, J. M.; Har, A. M.; Loutfy, R. O.; Eleryk, A. R. M. *Chem. Funct. Dyes* **1992**, *2*, 564.
(26) Grem, G.; Leditzky, G.; Ullrich, B.; Leising, G. *Adv. Mater.* **1992**, *4*, 36.
(27) (a) Zhang, C.; Braun, D.; Heeger, A. J. *J. Appl. Phys.* **1993**, *73*, 5177. (b) Vestweber, H.; Griener, A.; Lemma, U.; Mahrt, R. F.; Richert, R.; Heitz, W.; Bässler, H. *Adv. Mater.* **1992**, *4*, 661.
(28) Berggren, M.; Gustafsson, G.; Inganäs, O.; Andersson, M. R.; Wennerström, O.; Hjertberg, T. *Adv. Mater.* **1994**, *6*, 488.
(29) (a) Wu, C. C.; Sturm, J. C.; Register, R. A.; Tian, J.; Dana, E. P.; Thompson, M. E. *IEEE Trans. Electron Devices* **1997**, *44*, 1269. (b) Lamansky, S.; Kwong, R. C.; Nugent, M.; Djurovich, P. I.; Thompson, M. E. *Org. Electron.* **2001**, *2*, 53. (c) Lamansky, S.; Djurovich, P. I.; Abdel-Razzaq, F.; Garon, S.; Murphy, D. L.; Thompson, M. E. *J. Appl. Phys.* **2002**, *92*, 1570. (d) Vaeth, K. M.; Tang, C. W. *J. Appl. Phys.* **2002**, *92*, 3447. (e) Gong, X.; Robinson, M. R.; Ostrowski, J. C.; Moses, D.; Bazan, G. C.; Heeger, A. J. *Adv. Mater.* **2002**, *14*, 581. (f) Yang, X. H.; Neher, D.; Hertel, D.; Däubler, T. K. *Adv. Mater.* **2004**, *16*, 161. (g) Yang, X. H.; Neher, D. *Appl. Phys. Lett.* **2004**, *84*, 2476.
(30) (a) Förster, T. *Ann. Phys.* **1948**, *2*, 55. (b) Förster, T. *Discuss. Faraday Soc.* **1959**, 7.

(31) Jiang, C.; Yang, W.; Peng, J.; Xiao, S.; Cao, Y. *Adv. Mater.* **2004**, *16*, 537.
(32) Bulovic, V.; Shoustikov, A.; Baldo, M. A.; Bose, E.; Kozlov, V. G.; Thompson, M. E.; Forrest, S. R. *Chem. Phys. Lett.* **1998**, *287*, 455.
(33) Negres, R. A.; Gong, X.; Ostrowski, J. C.; Bazan, G. C.; Moses, D.; Heeger, A. J. *Phys. Rev. B* **2003**, *68*, 115209.
(34) List, E. J. W.; Creely, C.; Leising, G.; Schulte, N.; Schluter, A. D.; Scherf, U.; Müllen, K.; Graupner, W. *Chem. Phys. Lett.* **2000**, *325*, 132.
(35) Gong, X.; Ostrowski, J. C.; Moses, D.; Bazan, G. C.; Heeger, A. J. *Adv. Funct. Mater.* **2003**, *13*, 439.
(36) (a) Janietz, S.; Wedel, A. *Adv. Mater.* **1997**, *9*, 403. (b) Kim, C. H.; Shinar, J. *Appl. Phys. Lett.* **2002**, *80*, 2201. (c) Cocchi, M.; Virgili, D.; Giro, G.; Fattori, V.; Di Marco, P.; Kalinowski, J.; Shirota, Y. *Appl. Phys. Lett.* **2002**, *80*, 2401.
(37) Markham, J. P. J.; Samuel, I. D. W.; Lo, S. C.; Burn, P. L.; Weiter, M.; Bässler, H. *J. Appl. Phys.* **2004**, *95*, 438.

MA0494131